Electronic Supplementary Information for

Preparation and reactivity of a square-planar PNP cobalt(II)-hydrido complex: Isolation of the first {Co-NO}^{8}-hydride

V. Mahesh Krishnan, Hadi D. Arman, and Zachary J. Tonzetich*

Department of Chemistry, University of Texas at San Antonio, San Antonio, TX 78249
zachary.tonzetich@utsa.edu

Contents **Pages**

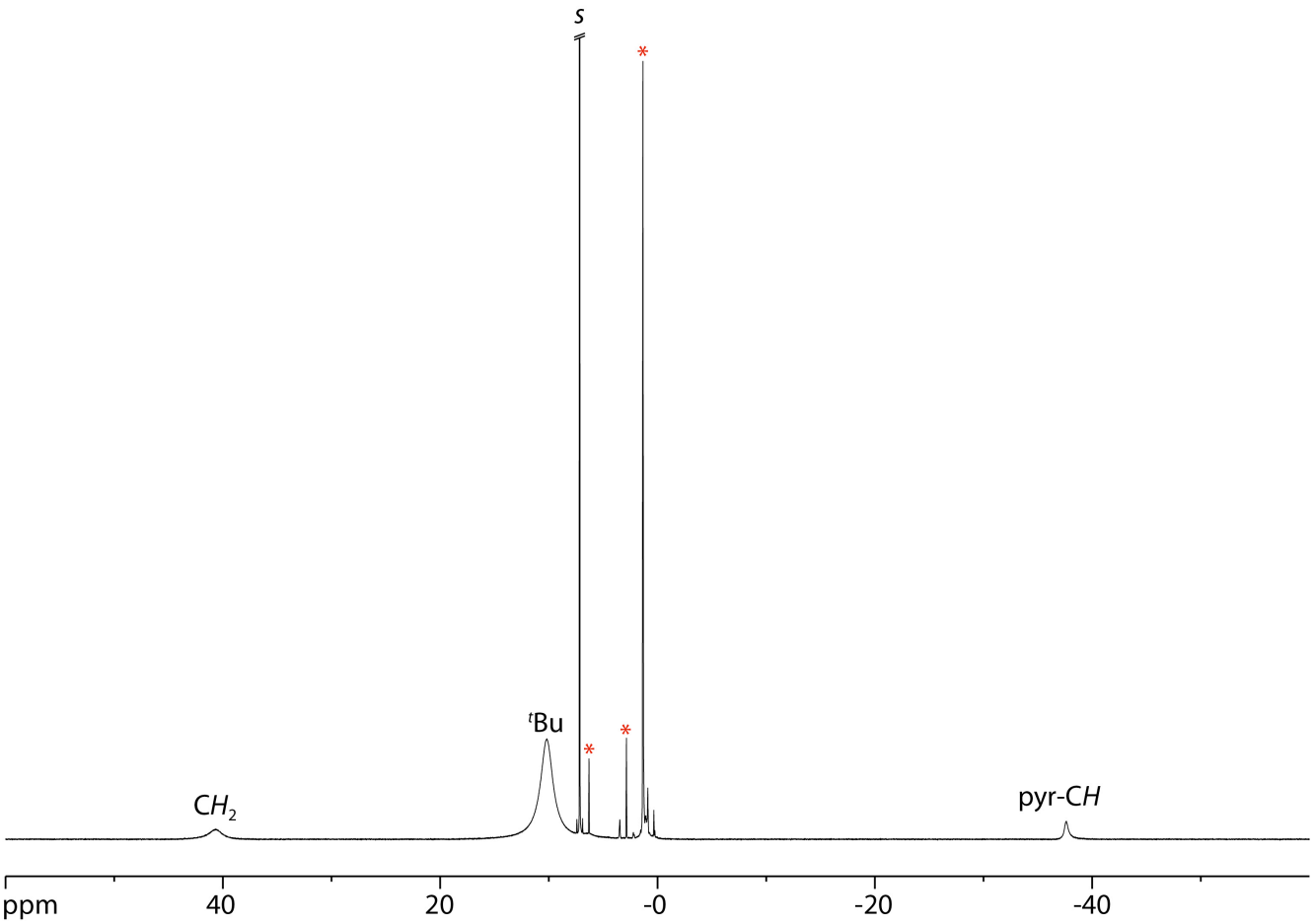

Figure S1. ^{1}H NMR spectrum of recrystallized **2-H** in benzene-d_6 (*s*). Asterisks denote resonances of **1-N$_2$**, which comprises ~25% of the sample according to peak integration.

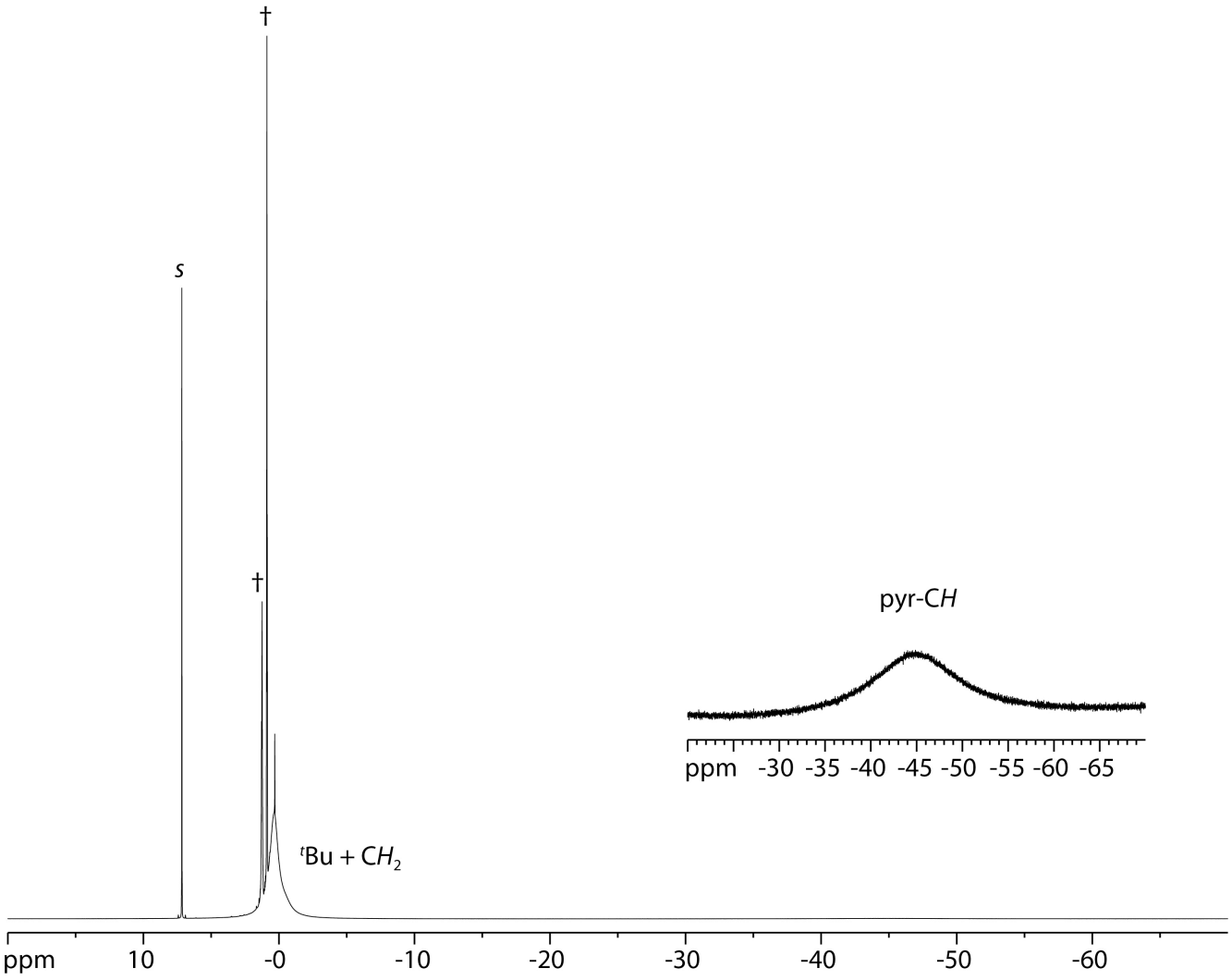

Figure S2. ^{1}H NMR spectrum of **2-BH$_4$** in benzene-d_6 (*s*). Crosses denote peaks due to residual pentane from recrystallization.

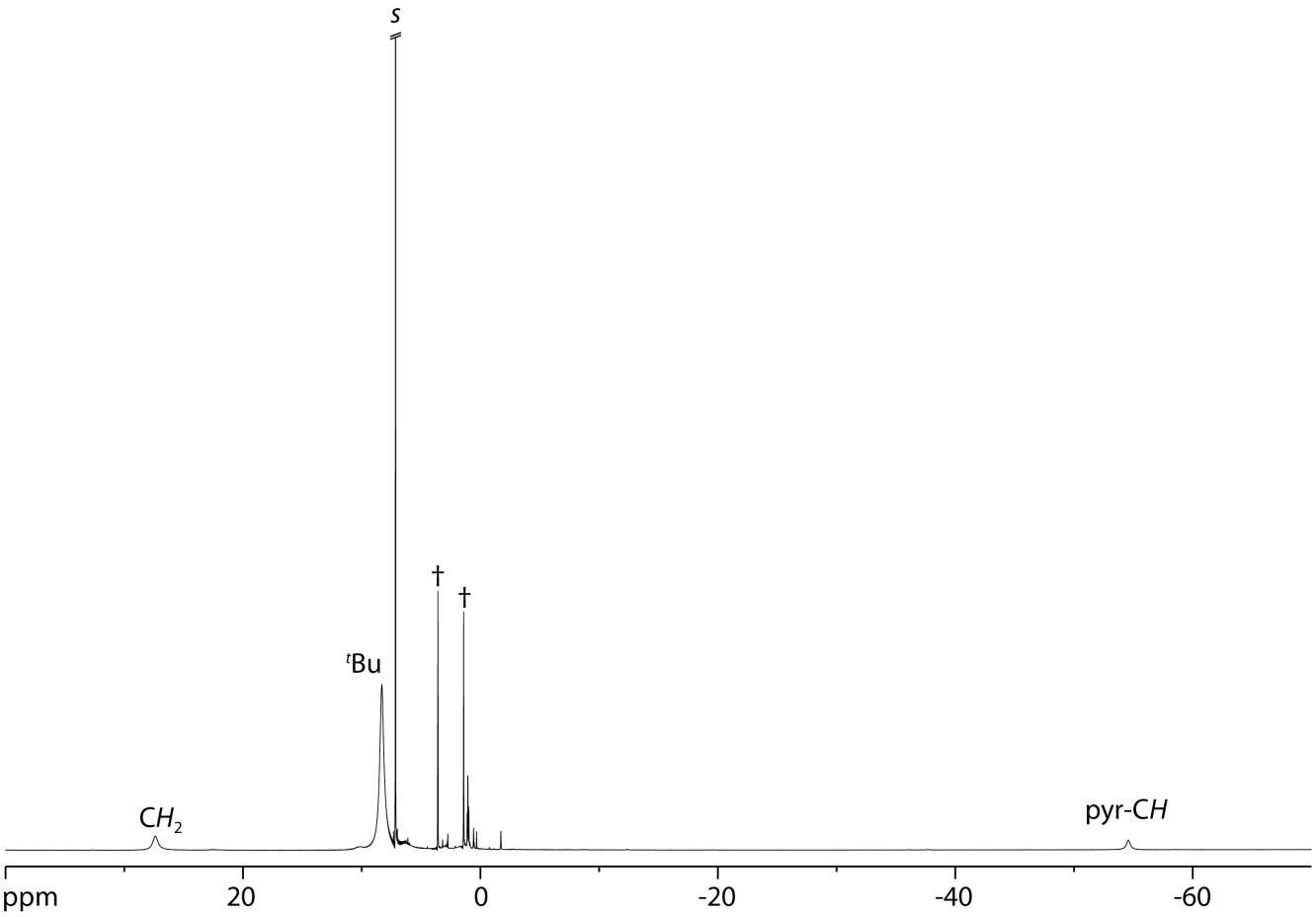

Figure S3. ^{1}H NMR spectrum of **2-O_2CH** in benzene-d_6 (*s*). Crosses denote peaks due to residual tetrahydrofuran.

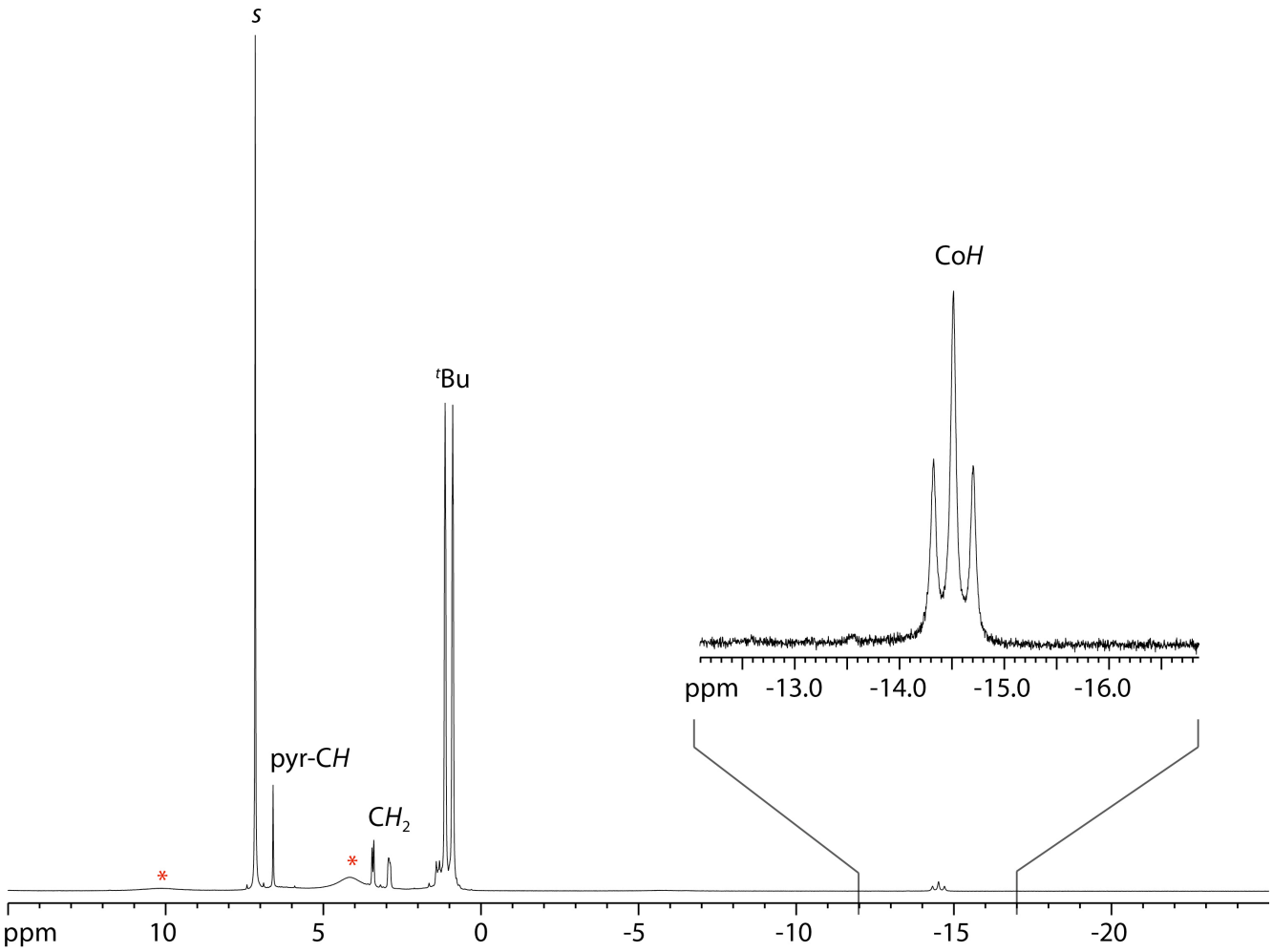

Figure S4. ^{1}H NMR spectrum of **1-NO(H)** in benzene-d_6 (*s*). Asterisk denote minor impurities arising from the presence of **1-N$_2$** in samples of **2-H** used to produce **1-NO(H)**.

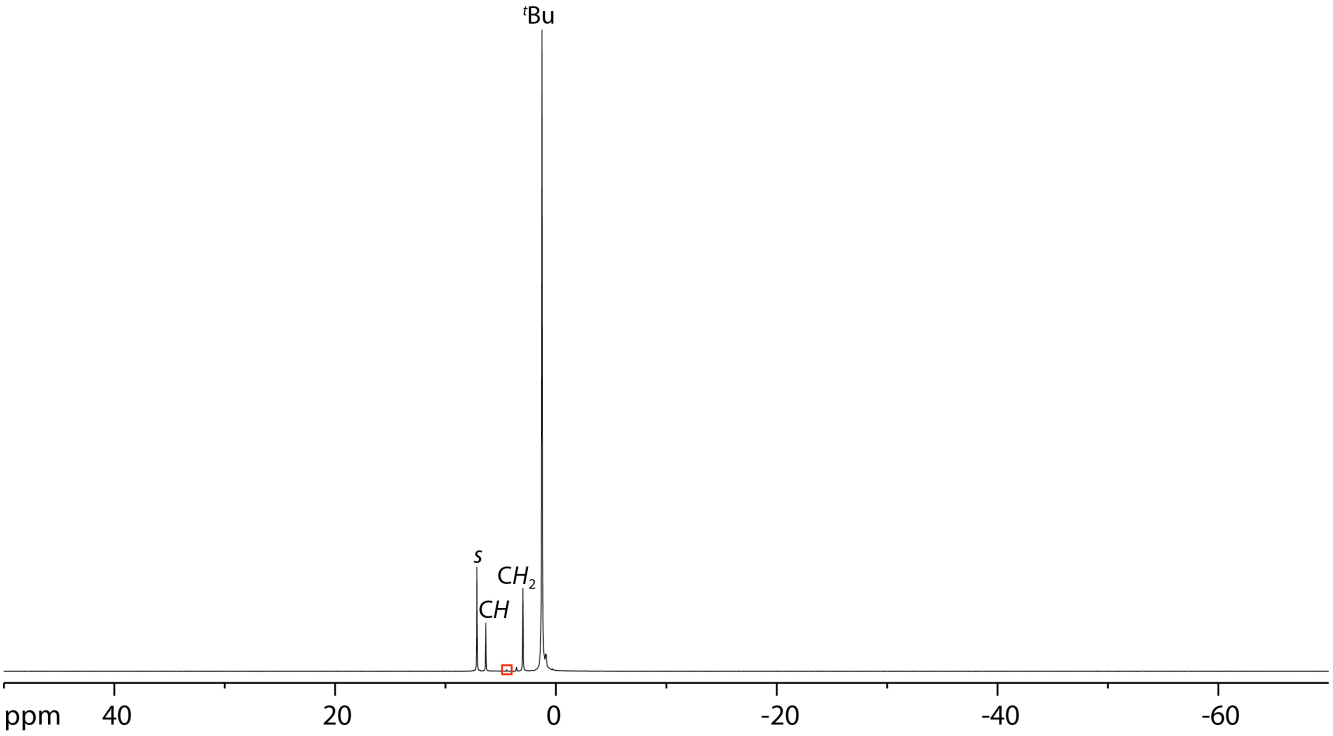

Figure S5. ^{1}H NMR spectrum of the reaction of **2-H** with CO in benzene-d_6 (*s*) The labeled peaks correspond to **1-CO**. The wide sweep width highlights the lack of any Co(II) species. The small resonance in the red box at 4.47 ppm corresponds to H_2, one of the byproducts of the reaction.

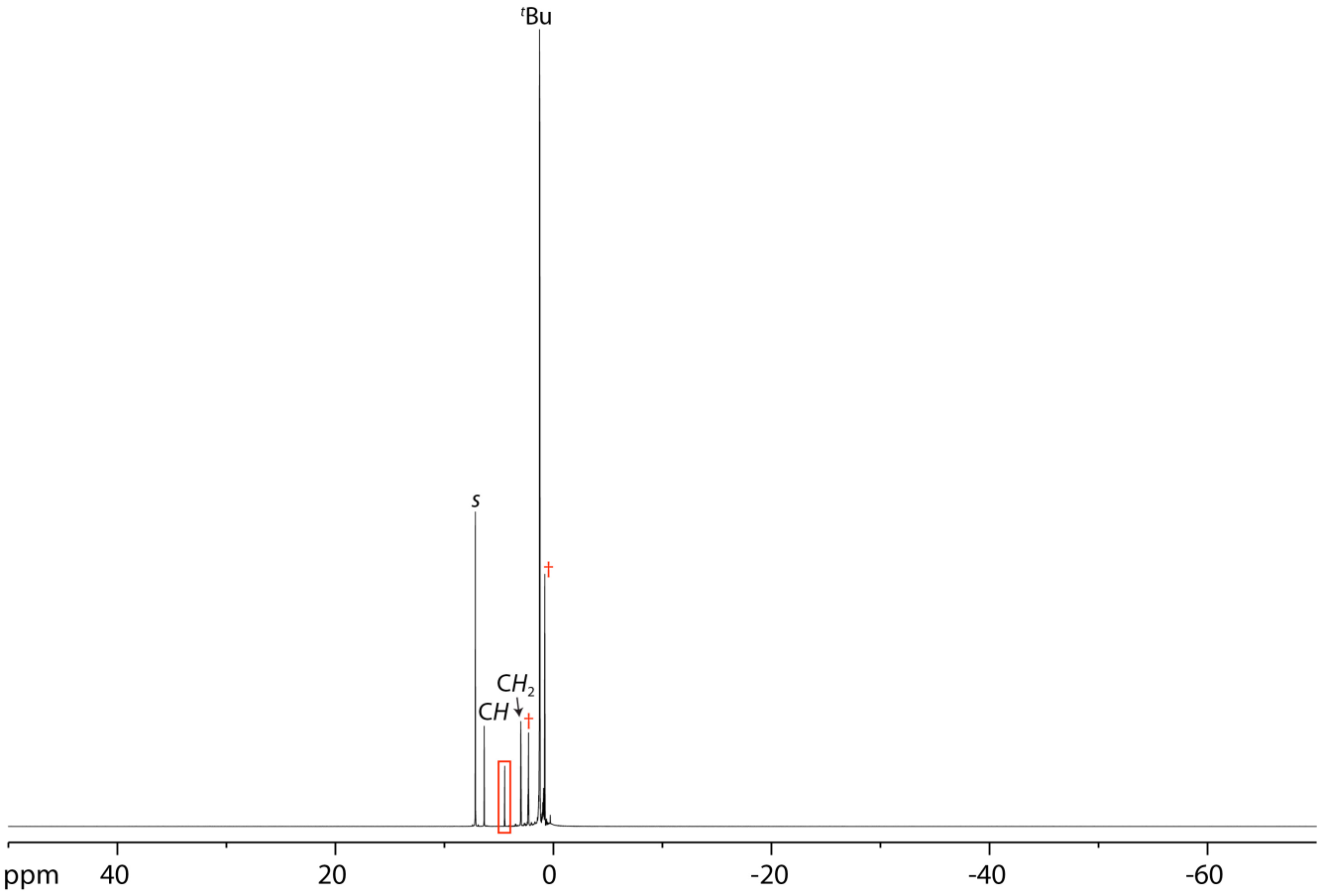

Figure S6. ^{1}H NMR spectrum of the reaction of **2-BH$_4$** with CO in benzene-d_6 (*s*) in the presence of Et_3N. The labeled peaks correspond to **1-CO**. The wide sweep width highlights the lack of any Co(II) species. The small resonance in the red box at 4.47 ppm corresponds to H_2, one of the byproducts of the reaction. The red crosses denote peaks for the other byproduct, $Et_3N{\cdot}BH_3$.

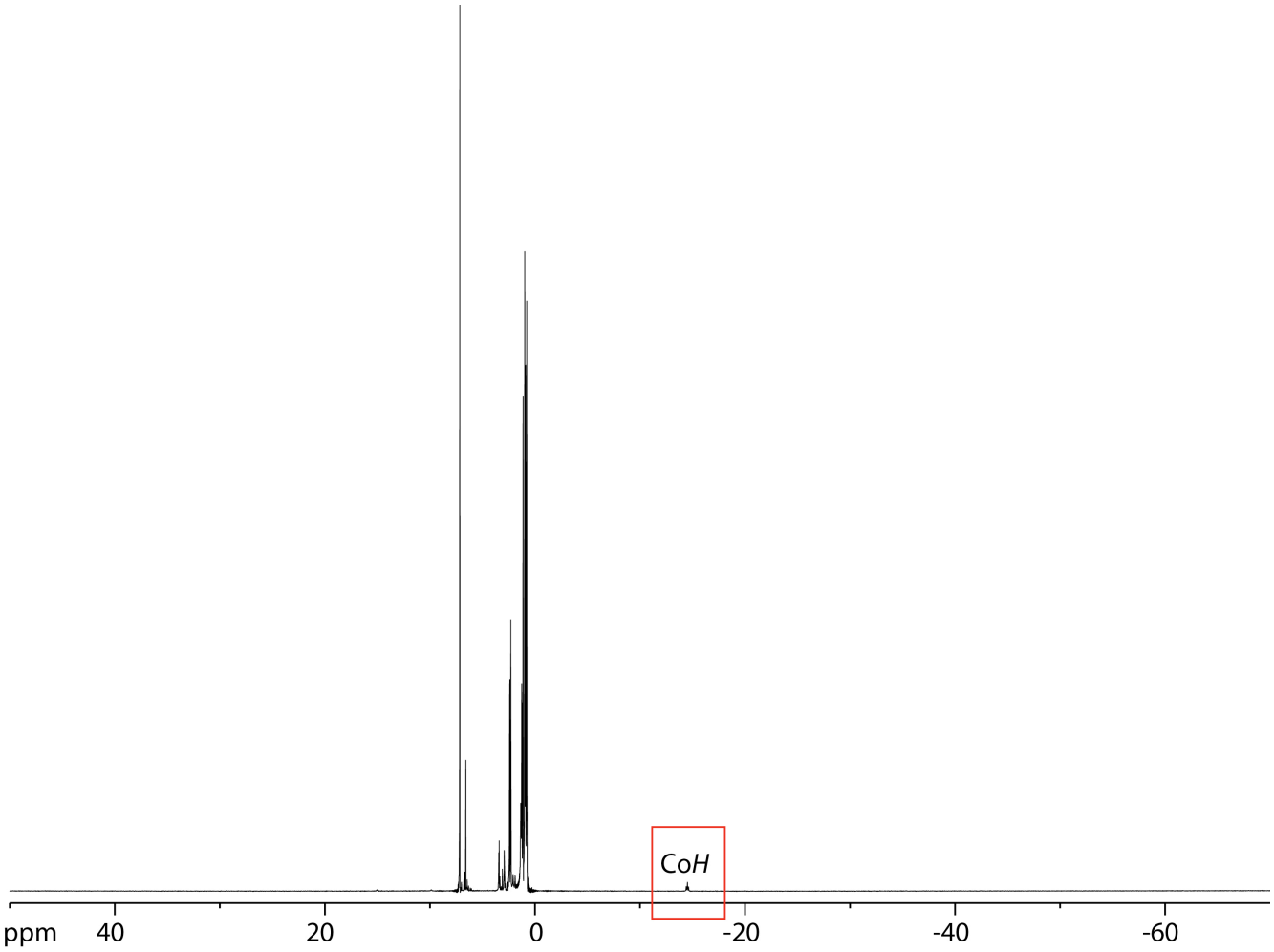

Figure S7. ^{1}H NMR spectrum of the reaction of **2-BH$_4$** with NO in benzene-d_6 (*s*) in the presence of Et_3N. The wide sweep width highlights the lack of any Co(II) species. The triplet resonance in the red box at –14.52 ppm corresponds to the hydride resonance of **1-NO(H)**.

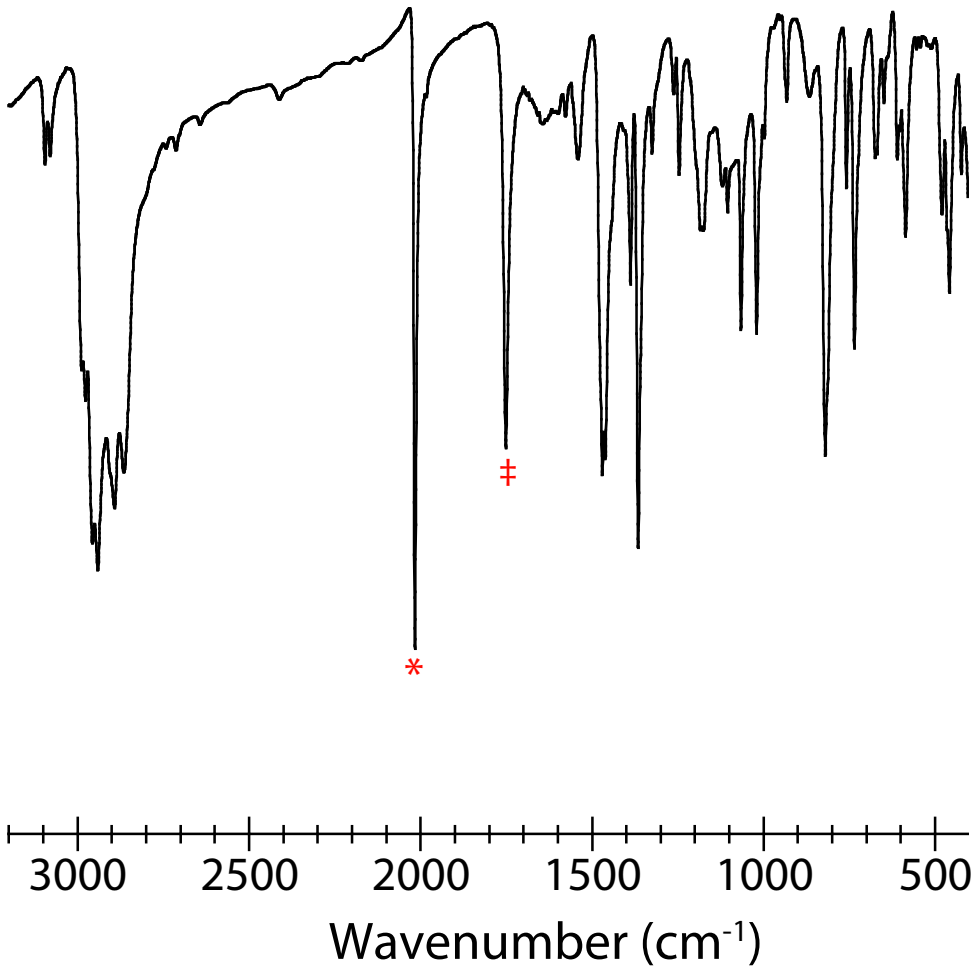

Figure S8. IR spectrum of **2-H** as a KBr pellet. The double dagger denotes the peak (1751 cm^{-1}) assigned to the Co-H stretch (compare Figure S11 below). The asterisk corresponds to the peak for the N-N stretch of the **1-N_2** impurity.

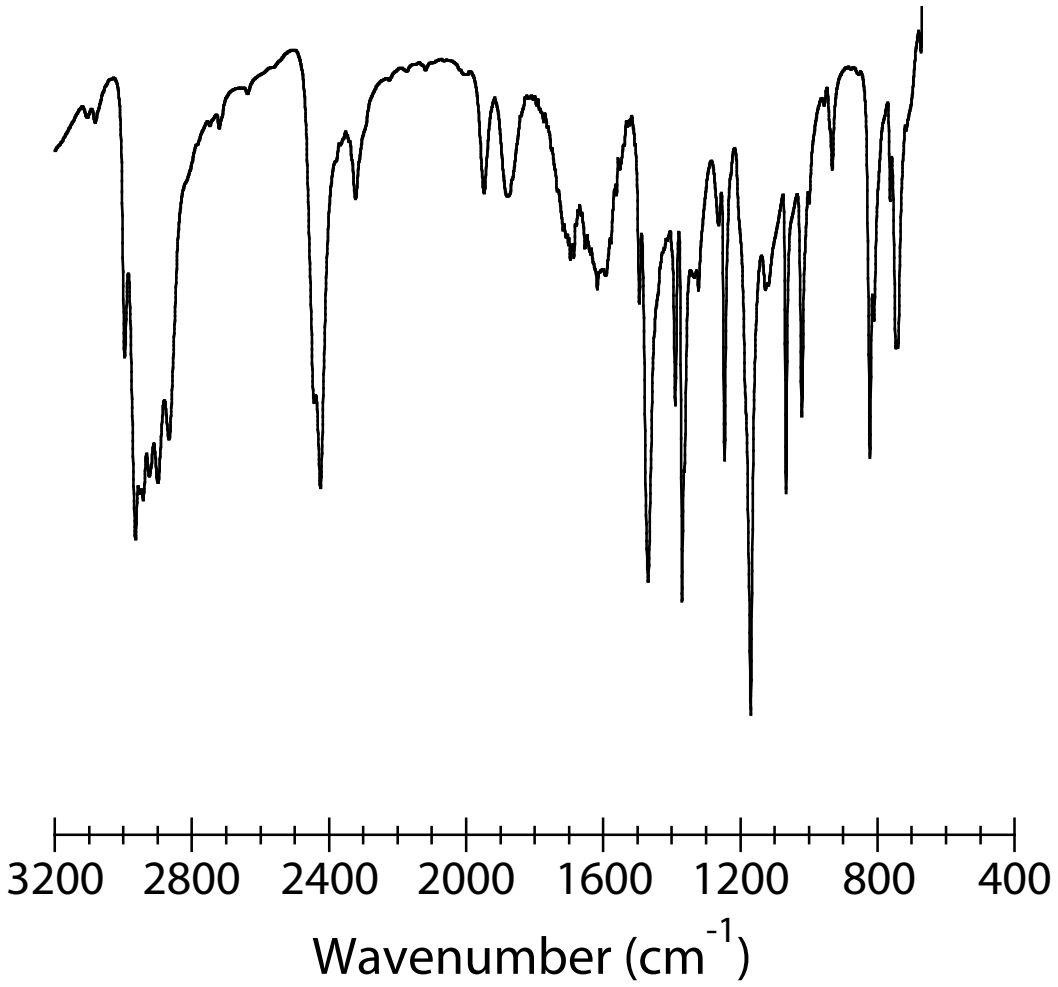

Figure S9. IR spectrum of **2-BH_4** as a KBr pellet.

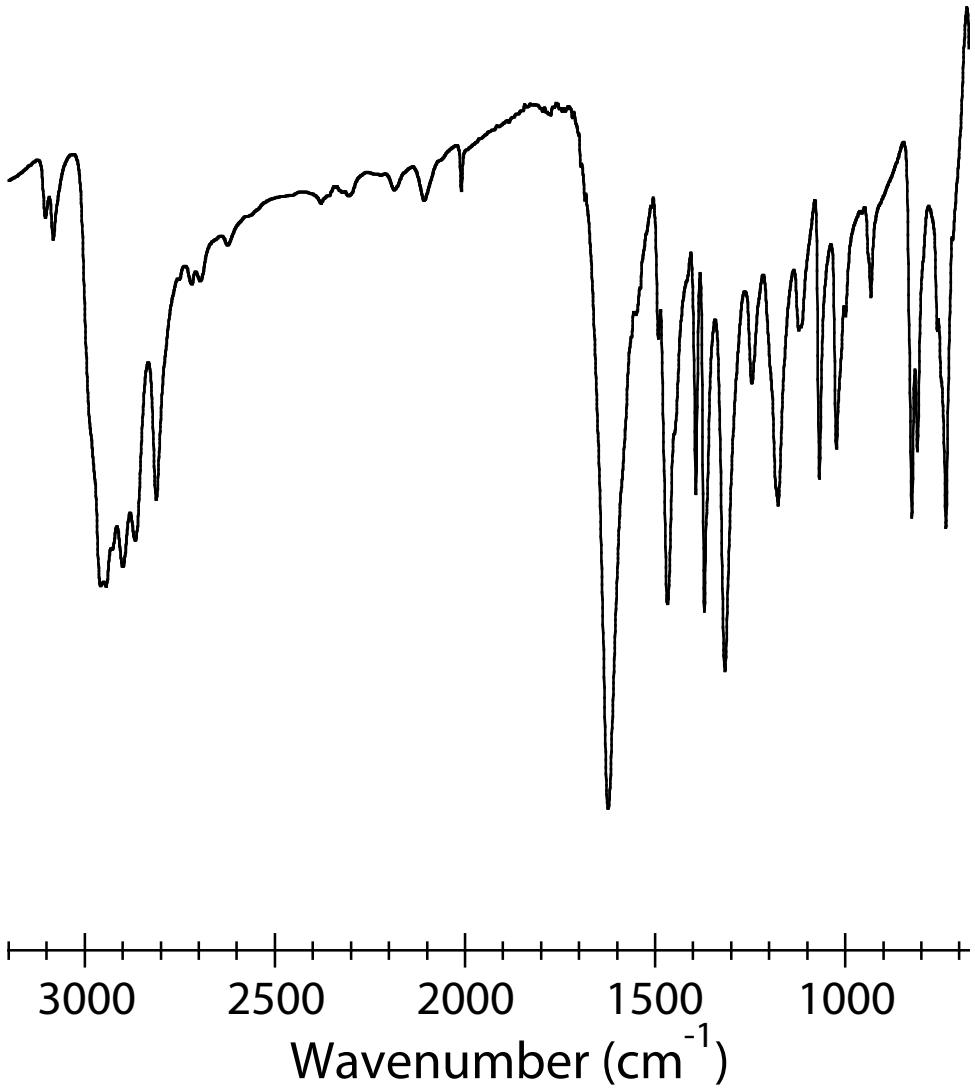

Figure S10. IR spectrum of **2-O_2CH** as a KBr pellet.

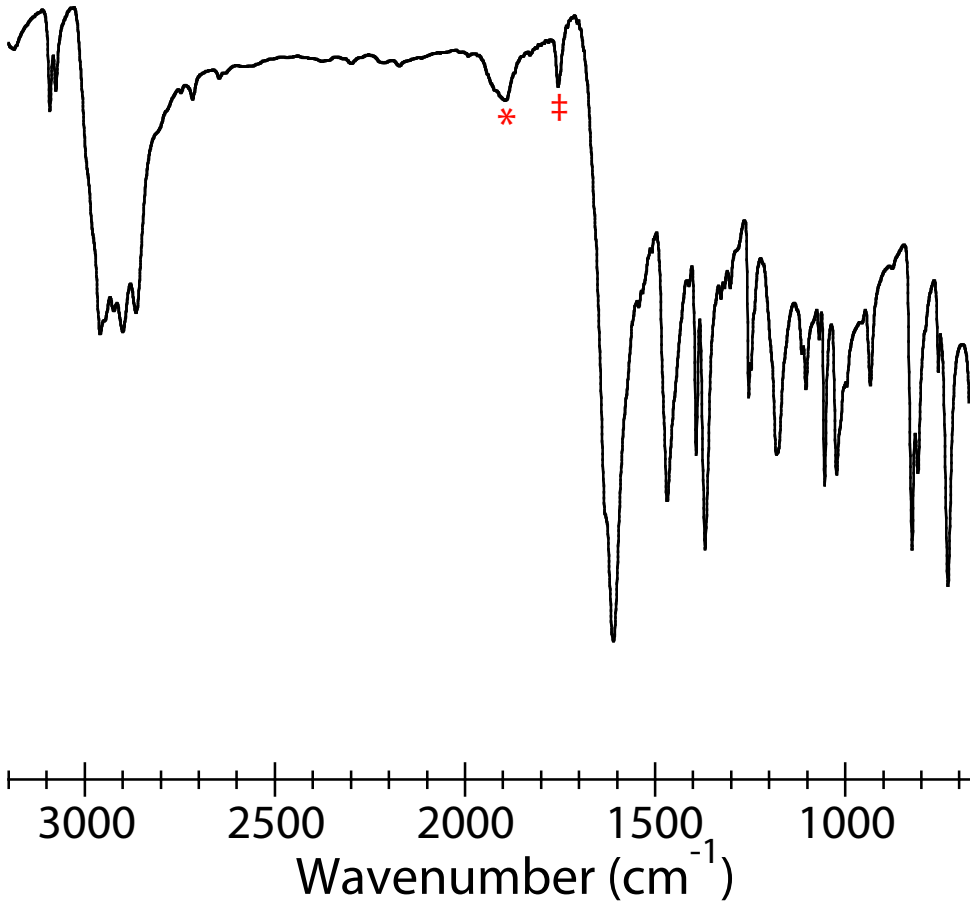

Figure S11. IR spectrum of **1-NO(H)** as a KBr pellet. The double dagger denotes the peak (1754 cm^{-1}) assigned to the Co-H stretch. The peak marked with an asterisk likely arises from an impurity attributable to the presence of **1-N_2** in the starting material.

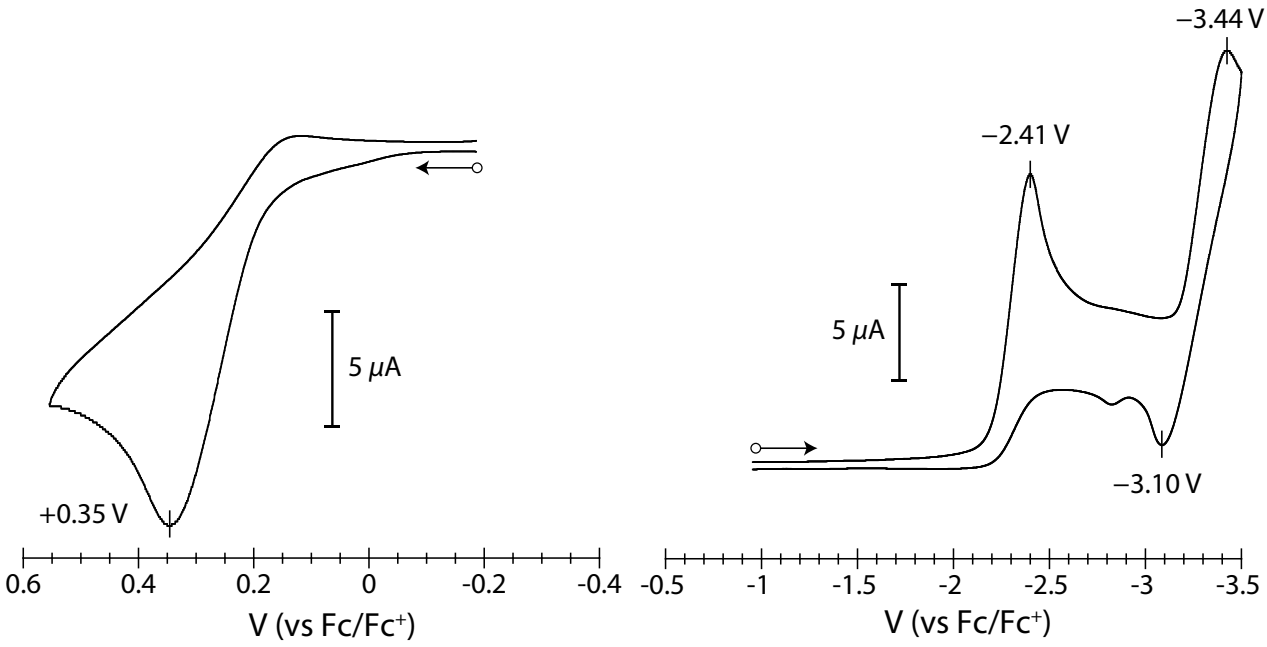

Figure S12. Cyclic voltammograms of **2-Cl** at a platinum electrode in tetrahydrofuran. The supporting electrolyte was 0.2 M Bu_4NPF_6 and the scan rate was 50 mV/s. The left panel displays the anodic sweep and the right displays the cathodic sweep.

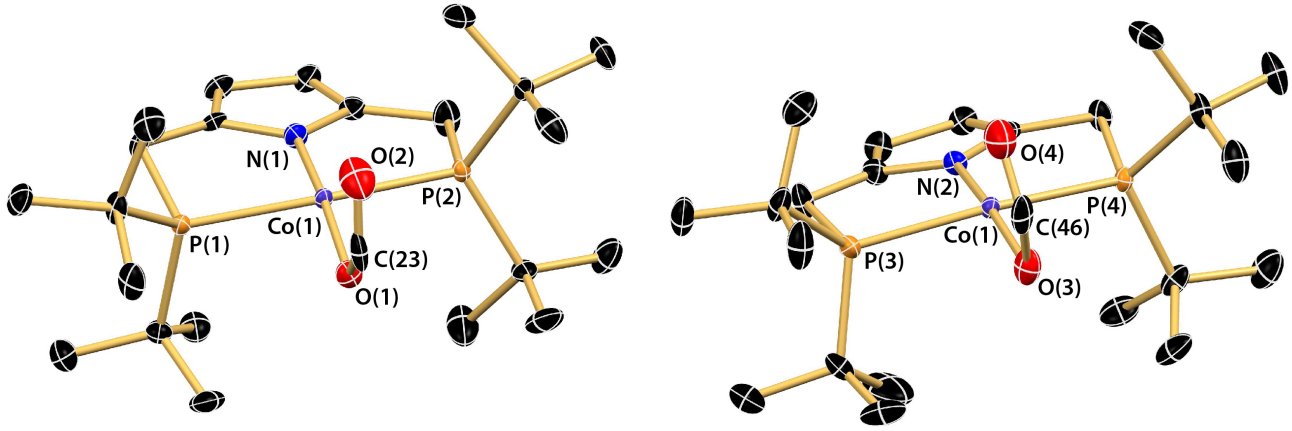

Figure S13. Thermal ellipsoid (50%) drawing of **2-O_2CH** showing both crystallographically-independent molecules in the asymmetric unit. Hydrogen atoms omitted for clarity.

Table S1. Crystallographic data and refinement parameters for **2-BH_4**, **2-O_2CH**, and **1-NO(H)**.[‡]

Compound	**2-BH_4**	**2-O_2CH**	**1-NO(H)**[†]
Empirical formula	$C_{22}H_{46}BCoNP_2$	$C_{23}H_{43}CoNO_2P_2$	$C_{22}H_{42}CoN_2OP_2$
Formula weight (g/mol)	456.28	486.45	471.44
Temperature (K)	98(2)	293(2)	98(2)
Crystal system, space group	Monoclinic $P2_1/n$	Monoclinic $P2_1$	Monoclinic $P2_1$
Unit cell dimensions (Å, deg)	a = 15.2602(10) b = 11.3904(6) c = 15.6393(12) β = 112.919(8)	a = 10.6498(4) b = 15.2862(5) c = 15.6734(6) β = 97.796(4)	a = 7.7482(3) b = 14.9473(8) c = 10.7812(6) β = 97.987(4)
Volume (Å^3)	2503.8(3)	2528.0(2)	1236.5(1)
Z	4	4	2
Calculated density (g/cm^3)	1.210	1.278	1.266
Absorption coefficient (mm^{-1})	0.821	0.824	0.838
F(000)	988	1044	506
Crystal size (mm)	0.40 × 0.07 × 0.03	0.33 × 0.17 × 0.07	0.40 × 0.23 × 0.07
Θ range	2.279 to 24.550º	2.345 to 25.050º	2.344 to 25.496º
Limiting indices	$-17 \le h \le 17$, $-13 \le k \le 12$, $-18 \le l \le 18$	$-12 \le h \le 12$, $-17 \le k \le 18$, $-18 \le l \le 18$	$-9 \le h \le 9$, $-17 \le k \le 18$, $-13 \le l \le 12$
Reflections collected / unique	24839 / 4185 [R_{int} = 0.0441]	51235 / 8784 [R_{int} = 0.0739]	13323 / 4528 [R_{int} = 0.0304]
Completeness to Θ	99.9%	99.9%	99.9%
Absorption correction	multi-scan ABSCOR	multi-scan ABSCOR	multi-scan ABSCOR
Min. and max transmission	0.754 and 1.000	0.629 and 1.000	0.858 and 1.000
Data / restraints / parameters	4185 / 6 / 223	8784 / 1 / 547	4528 / 1 / 265
Goodness-of-fit on F^2	1.109	1.094	1.094
Final R indices [$I > 2\sigma(I)$]	R_1 = 0.0887, wR_2 = 0.1679	R_1 = 0.0471, wR_2 = 0.0937	R_1 = 0.0340, wR_2 = 0.0782
R indices (all data)	R_1 = 0.0909, wR_2 = 0.1690	R_1 = 0.0487, wR_2 = 0.0944	R_1 = 0.0347, wR_2 = 0.0785
Largest diff. peak and hole (e·Å^{-3})	0.967 and −0.946	0.484 and −0.434	0.910 and −0.518

[‡]Refinement method was full-matrix least-squares on F^2; wavelength = 0.71073 Å. $R_1 = \sum||F_o|-|F_c||/\sum|F_o|$; $wR_2 = \{\sum[w(F_o^2-F_c^2)^2]/\sum[w(F_o^2)^2]\}^{1/2}$.
[†]The hydride ligand could not be located in the difference map and was therefore not included in the refinement.